

A Wound-Healing Assay Based on Ultraviolet Light Ablation

Shang-Ying Wu¹, Yung-Shin Sun², Kuan-Chen Cheng³, and Kai-Yin Lo¹

Abstract

Collective cell migration plays important roles in many physiological processes such as embryonic development, tissue repair, and angiogenesis. A “wound” occurs when epithelial cells are lost and/or damaged due to some external factors, and collective cell migration takes place in the following wound-healing process. To study this cellular behavior, various kinds of wound-healing assays are developed. In these assays, a “wound,” or a “cell-free region,” is created in a cell monolayer mechanically, chemically, optically, or electrically. These assays are useful tools in studying the effects of certain physical or chemical stimuli on the wound-healing process. Most of these methods have disadvantages such as creating wounds of different sizes or shapes, yielding batch-to-batch variation, and damaging the coating of the cell culture surface. In this study, we used ultraviolet (UV) lights to selectively kill cells and create a wound out of a cell monolayer. A comparison between the current assay and the traditional scratch assay was made, indicating that these two methods resulted in similar wound-healing rates. The advantages of this UV-created wound-healing assay include fast and easy procedure, high throughput, and no direct contact to cells.

Keywords

wound-healing assay, collective cell migration, ultraviolet light

Introduction

Collective cell migration is an important cellular event involved in many different physiological processes such as embryonic development, tissue repair, angiogenesis, and wound healing.^{1–3} Recently, it was suggested that this collective behavior plays a crucial role in the invasion and spread of malignant cells.^{4–6} When cells migrate collectively, they often form the so-called self-assembled monolayers where cells are attached to each other in mechanical and biochemical ways. This complicated phenomenon occurs in cell proliferation, cell-cell communication, and cell-microenvironment interaction. To follow the dynamic process of collective cell migration, researchers have developed a number of different *in vitro* techniques, including wound-healing assays.^{7–11} These assays are commonly and widely used because they are economical and easy to use, and the shape of cells as well as the wound-healing rate can be easily observed.

In a wound-healing experiment, it is essential to create a cell-free region in a cell monolayer. Introducing this cell-free region could cause various cellular responses such as cell growth and cell migration.^{12,13} These behaviors can be directly observed using time-lapse microscopes, and subsequently the wound-healing rate can be analyzed. Two types of wound-healing assays have been widely and commonly used: the scratch wound-healing assay and the barrier wound-healing assay.

The procedure of a scratch wound-healing assay includes seeding cells to grow into a confluent monolayer, using a tip to scratch a certain area, and allowing cells to repopulate the gap.^{14–16} Essen BioScience (Ann Arbor, MI) has commercialized the scratch assay, called the CellPlayer Migration Assay. There are many advantages regarding this method, such as (1) it can be applied in any substrate, (2) cells move in a certain direction (to close the wound), and (3) the morphology and migration of cells can be observed and recorded to calculate the displacement and rate.¹⁷ However, using tips to mechanically create wounds makes the size and shape of the cell-free region difficult to control from experiment to experiment. Also, scratching could damage the coating of the cell culture surface and cause incorrect results. Instead, the barrier wound-healing assay is more

¹Department of Agricultural Chemistry, National Taiwan University, Taipei, Taiwan

²Department of Physics, Fu-Jen Catholic University, New Taipei City Taiwan

³Graduate Institute of Food Science Technology, National Taiwan University, Taipei, Taiwan

Received March 14, 2016.

Corresponding Author:

Kai-Yin Lo, Department of Agricultural Chemistry, National Taiwan University, 1 Sec. 4, Roosevelt Road, Taipei 10617, Taiwan.
Email: kaiyin@ntu.edu.tw

applicable in cell migration studies because it maintains surface integrity using a stopper (barrier) to keep cells away from the wound area.^{18,19} It has been reported that this method results in similar wound-healing responses compared to scratch wound-healing assays.^{20–22}

The procedure of a barrier wound-healing assay includes putting the stopper onto the substrate, seeding cells to grow into a confluent monolayer, removing the stopper, and allowing cells to repopulate the gap. Commercial barrier-type assays also have been developed, including cell migration stoppers from Platypus Technologies (Madison, WI) and cell culture inserts from Ibidi (Martinsried, Germany). Basically, cell stoppers are placed inside each well of a 96-well plate to create cell-free areas.

Given the drawbacks of the scratch assay, laser photoablation and electrical wound-healing assays have been developed as substitutes.^{23,24} Currently, laser is the only optical method to create wounds. It can indirectly cause photothermal, photochemical, and photomechanical effects, which lead to cell damage and death. The size of the wound can be well controlled for good experimental repeatability. Moreover, wounds of any shape can be produced, and observation of cell migration can be automated via optical fibers and microscopes. Zordan et al.²³ developed a high-throughput wound-healing assay using the laser-enabled analysis and processing (LEAP) instrument to create reproducible wounds in each well of a 96-well plate. This system then records bright-field images of each well at a given time interval. In the electrical wound-healing assay, cells growing on electrodes are subjected to currents, resulting in severe electroporation and subsequent cell death. The wound-healing process is monitored using the electric cell-substrate impedance sensing (ECIS) technology.²⁴ Applied BioPhysics (Troy, NY) has commercialized the electrical assay called the ECIS Electroporation and Wounding Module.

Cell migration is possibly due to the influence of the cell-free region, where the surface tension sensed by cells changes. Murrell et al.²⁵ reported using microfluidic chips to create a wound-healing assay. In this assay, trypsin, a proteolytic enzyme, was used to rupture cells and create a wound in about 5 min. It was found that cells with a density of 2000 to 3000 cells/mm² failed to restore back to a monolayer, but the wound-healing rate was fast. On the other hand, cells with a higher density of greater than 3000 cells/mm² could recover into a complete monolayer but with a slow healing rate.

In this study, we report a wound-healing assay based on ultraviolet (UV) light ablation. Depending on the wavelength, UV lights can be divided into UVA (315–400 nm), UVB (280–315 nm), and UVC (100–280 nm). Both UVB and UVC were shown to induce apoptosis of fibroblasts and skin keratinocytes.^{26–29} Matta et al.³⁰ studied the threshold doses and environmental UVA and UVB exposure times

necessary to produce apoptosis and necrosis in human fibroblasts. A threshold dose between 24 and 28 kJ/m² was found to induce apoptosis and necrosis, and this value corresponded to 19 and 23 min of environmental UVA and UVB exposure, respectively, at solar noon in Puerto Rico. Here in this report, using a customized mask, we were able to create a cell-free region out of a cell monolayer by well controlling the UV exposure dose. This UV wound-healing assay resulted in similar wound closure responses compared to the scratch assay, and it provides many advantages such as fast, easy procedure and high throughput. Moreover, both the scratch assay and the barrier assay require direct contact to immobilized cells,^{5,31} meaning that these two assays are limited to “open” systems. In the current UV assay, cells can be cultured within a “closed” system made of transparent materials such as glass or plastic, making this assay compatible with microfluidic devices for further cellular studies.^{32–34}

Materials and Methods

UV Wound-Healing Assay

The bottom of a 35-mm petri dish (Mattek Corp., Ashland, MA) was covered by a mask with a desired pattern. NIH3T3 cells, purchased from Bioresource Collection and Research Center (BCRC, Hsinchu, Taiwan), were trypsinized and resuspended in Dulbecco's modified Eagle's medium (DMEM; Gibco, Waltham, MA) containing 10% calf serum (CS; Invitrogen, Carlsbad, CA). Then, 5×10^5 cells were passed to a 35-mm dish and exposed to the UV light source (UVP, Upland, CA). The intensity was measured using a power meter specified for UV lights (Teledyne, Thousand Oaks, CA). After UV exposure, the dish was transferred to an incubator under 37 °C and 5% CO₂ overnight. Then the medium was changed, and the shape and size of the wound were observed using an inverted microscope (ESPA, Hsinchu, Taiwan) under different conditions such as wavelength, intensity, and exposure period. Chemicals β -lapachone and honokiol were purchased from Sigma (St. Louis, MO). Detailed steps are indicated in **Figure 1A** (left).

Scratch Wound-Healing Assay

A total of 5×10^5 NIH3T3 cells were cultured with DMEM + 10% CS in a 35-mm petri dish placed inside an incubator under 37 °C and 5% CO₂ overnight. Then a pipette tip was used to scratch the cells and create the wound. Detailed steps are indicated in **Figure 1A** (right).

Viability Assay

The cleavage of yellow tetrazolium salt MTT (3-[4,5-cimethylthiazol-2-yl]-2,5-diphenyl tetrazolium bromide) (Sigma, St.

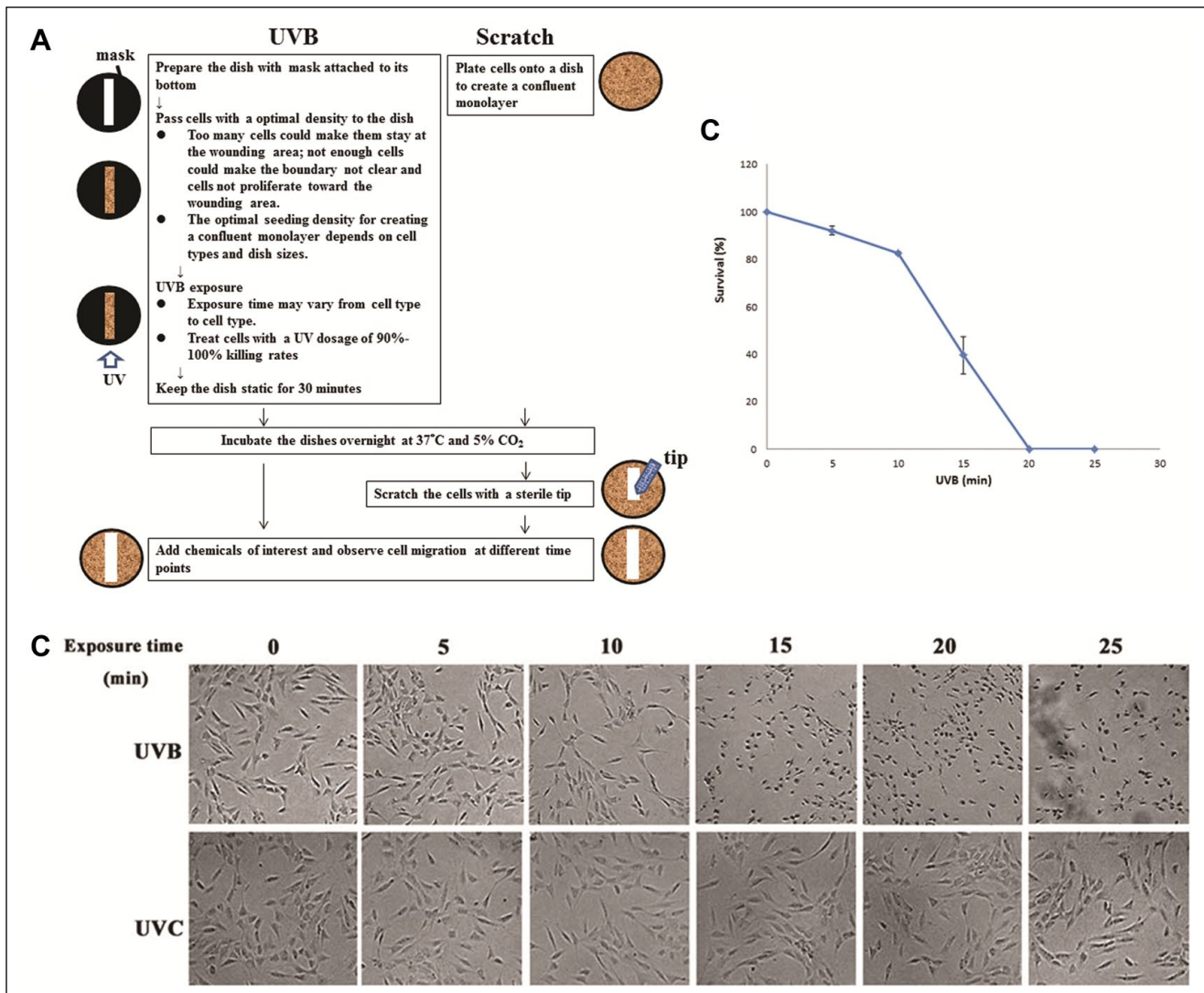


Figure 1. (A) Detailed steps in the UV wound-healing assay (left) and the scratch wound-healing assay (right). (B) NIH3T3 cells cultured in dishes were exposed to UVB (top) or UVC (bottom) for various time periods. (C) Cell viability assay shows the survival rate after UVB exposure.

Louis, MO) to purple formazan crystal by live cells can be used for quantification of cell proliferation and viability. In the viability assay, cells were passed to a 24-well microplate and exposed to the UV light for different exposure periods. Then, 40 μ L MTT solution (5 mg/mL in phosphate-buffered saline [PBS]) was added to each well, and the incubation took 2 h at 37°C. Then 400 μ L of solubilization solution, DMSO, was added to the wells for a 15-min incubation. Finally, the absorbance was measured by the enzyme-linked immunosorbent assay plate reader (Tecan, Männedorf, Switzerland) at 590 nm.

Calculation of Wound-Healing Rate

We observed cell migration (i.e., wound healing) inside each culture area (a petri dish or wells of a microplate) using a

bright-field inverted microscope (ESPA, Hsinchu, Taiwan). Time-lapse images were taken at an interval as specified in the context. Images were further analyzed using ImageJ, which is a free Java-based software developed by the National Institutes of Health (NIH, Bethesda, MD). This software was used to draw the wounding boundaries by determining the threshold between high-cell density and low-cell density areas. These boundaries could be easily drawn before 24 h. However, it became difficult to locate these lines after 24 h because cells grew to cover almost all the initially cell-free areas. Therefore, the wound-healing rates, indicating the progressing of the wounding boundaries, were calculated based on wound closure within the first 24 h. For each experimental condition, three independent runs were performed to get the standard error of the mean (SEM).

Table 1. Original and Transmitted Output Powers of UVB and UVC through Selective Dishes and Microplates.

Culture Dish	Brand	UVB		UVC	
		Output (mW/cm ²)	Transmission Rate, %	Output (mW/cm ²)	Transmission Rate, %
—	—	4.7	—	5.35	—
10-cm dish	—	2.1	45	0.07	1.3
35-mm dish	Mattek Corp. (Ashland, MA)	1.6	34	0.055	1.0
24-well plate	NEST Biotech (jiangsu, China)	1.2	26	0.03	0.5

The transmission rate is calculated as (transmitted power)/(original power) in %.

Results and Discussion

Use UVB for Creating Wounds

The wavelength of UVB ranges from 280 to 315 nm, and that of UVC ranges from 100 to 280 nm. As shown in **Table 1**, compared to UVB, UVC has a relatively stronger output intensity but a much lower transmission rate to petri dishes and microplates. The output power of the UVB light source is about 4.7 mW/cm². After being blocked by dishes or wells of a microplate, the transmitted intensity decreased to 1 to 2 mW/cm², corresponding to transmission rates of about 26% to 45%. For the UVC light source, while the output power is 5.35 mW/cm², almost 99% of the power was blocked by dishes or wells.

NIH3T3 fibroblasts were cultured inside wells of a 24-well microplate and were exposed to UVB or UVC light sources. As shown in **Figure 1B** (top), almost all cells were killed after a 20-min exposure of UVB. The total energy required to kill these cells was calculated to be around 1.44 J/cm². On the other hand, UVC did not cause any detrimental effects to cells even after a 25-min irradiation, as indicated in **Figure 1B** (bottom). The viability assay, shown in **Figure 1C**, indicated that almost all cells were killed after a UVB exposure of 20 min.

To find out the optimal exposure condition, we tried to kill cells in two ways. In the first manner, cells cultured overnight and attached to the dish surface were exposed to UVB. It turns out that once cells formed a monolayer, they appeared dark and adhered tightly to the dish after UVB exposure. It was then difficult to remove these dead cells by simply washing with PBS or trypsin of low concentration, probably due to the UV-induced crosslinking between cells and surface coatings of dishes. In the second manner, cells were exposed to UVB for 20 min at the suspension stage and were allowed to settle down afterward. Meanwhile, the culture dish was kept static for half an hour to let viable cells attach to the surface and avoid non-adherent cells floating to the wounded area. Then the dish was transferred to an incubator for an overnight incubation. Under such conditions, dead cells were removed easily and the wounded area was clear for observation. As a result, the second method was used in the following experiments.

Wounds Created by UVB Exposure

To create a wound, the bottom of a 35-mm petri dish was masked with tape of a 1-mm gap located at the center. Then, 5×10^5 NIH3T3 cells were seeded inside the dish, exposed to UVB for 20 min (total received energy ~ 1.92 J/cm²), and kept static inside an incubator overnight (see **Fig. 2A**). For comparison, a traditional scratch method was used to create wounds. NIH3T3 cells were trypsinized and passed to a 35-mm dish for culture overnight. A wound size of about 1 mm in width was created by scratching the cell monolayer with a 1-mL tip (see **Fig. 2B**). The scratch method created a wound of a clear area and well-defined boundaries, while in the UV method, few cells remained at the center and the edges were somehow irregular, possibly due to some nonadherent cells floating to the UV-exposed area and settling down.

Still, the UV wound-healing assay has many advantages over the scratch assay, such as it is fast, easy, and capable of high-throughput screening. Using this method, wounds of different sizes and shapes can be created simply by changing the mask to desired patterns. To demonstrate this, we created a circular wound 2-mm in diameter and a 1-mm \times 1-mm square wound by simply placing double-sided tapes (thickness = 0.07 mm; 3M, St. Paul, MN) of corresponding patterns on the bottom of petri dishes. The cell culture dishes were exposed to UVB for 20 min, and clear wounds were then created as shown in **Figure 2C**. Such double-sided tapes provide great flexibility in creating wounds of different sizes and shapes because they can be easily processed to required patterns with commercial cutting machines such as a CO₂ laser scribe. Wounds of different geometry shapes could also be attained in the barrier assay³⁵ or the laser ablation.²³

The initial seeding density is critical in creating wounds. If not enough cells were seeded, the space among cells could make them proliferate but not migrate toward the wounding area (**Fig. 2D**, top). On the other hand, if the seeding density is too high, cells could remain in the wounding area, possibly due to sedimentation of those floating cells (**Fig. 2D**, bottom). In the current case, an optimal density of 5×10^5 cells was obtained for a 35-mm dish (**Fig. 2D**, middle).

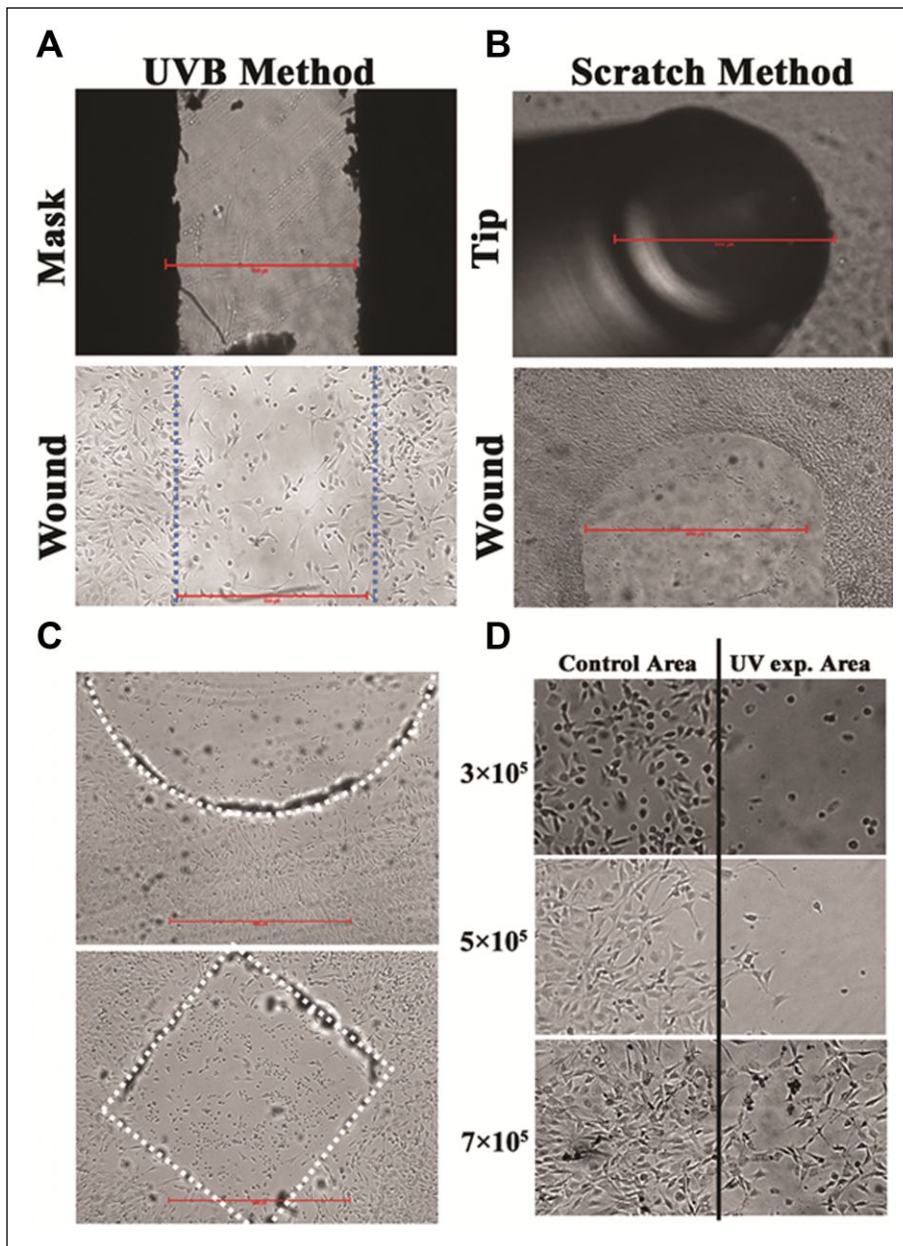


Figure 2. Wounds created by (A) the UVB method and (B) the scratch method. Scale bar = 1 mm. (C) Wounds of different shapes (top: a circle; bottom: a square) were created using the UVB method. Scale bar = 1 mm. (D) Different seeding densities in the 35-mm dish for creating wounds using the UVB method. From top to bottom: 3×10^5 cells, 5×10^5 cells, and 7×10^5 cells. Left: control areas (without UVB exposure). Right: wounding areas (with UVB exposure).

Comparison of Wound-Healing Rates in Scratch and UV Methods

To compare the wound-healing rates in scratch and UV methods, wounds of 1 mm in width were created using these two methods. Different concentrations of honokiol were added to different wells for observing their effects on wound-healing rates. Honokiol, a compound isolated from species of *Magnolia*, was reported to inhibit cell migration in a dose-dependent manner.^{36,37} Time-lapse images were taken at an interval of 12 h for 36 h, as shown in **Figure 3A** (top: scratch method; bottom: UV method). As shown in **Figure 3B**, using either of these two methods, wound-healing rates

decreased with increasing concentrations of honokiol, and the rates were comparable in these two methods. For example, in both methods, the wound-healing rates decreased from 16 $\mu\text{m}/\text{h}$ without adding honokiol to 11 $\mu\text{m}/\text{h}$, 11 $\mu\text{m}/\text{h}$, and 6 $\mu\text{m}/\text{h}$ after adding honokiol of 10 μM , 20 μM , and 40 μM , respectively.

This UV method was also used to test the effect of β -lapachone, a derivative of naturally occurring lapachol, on the wound-healing process. It has been reported that a low concentration of β -lapachone accelerated the proliferation and migration of NIH3T3 fibroblasts via extracellular signal-regulated kinase (ERK) and p38 signaling pathways.³⁸ Using the UV method, the wound-healing rate

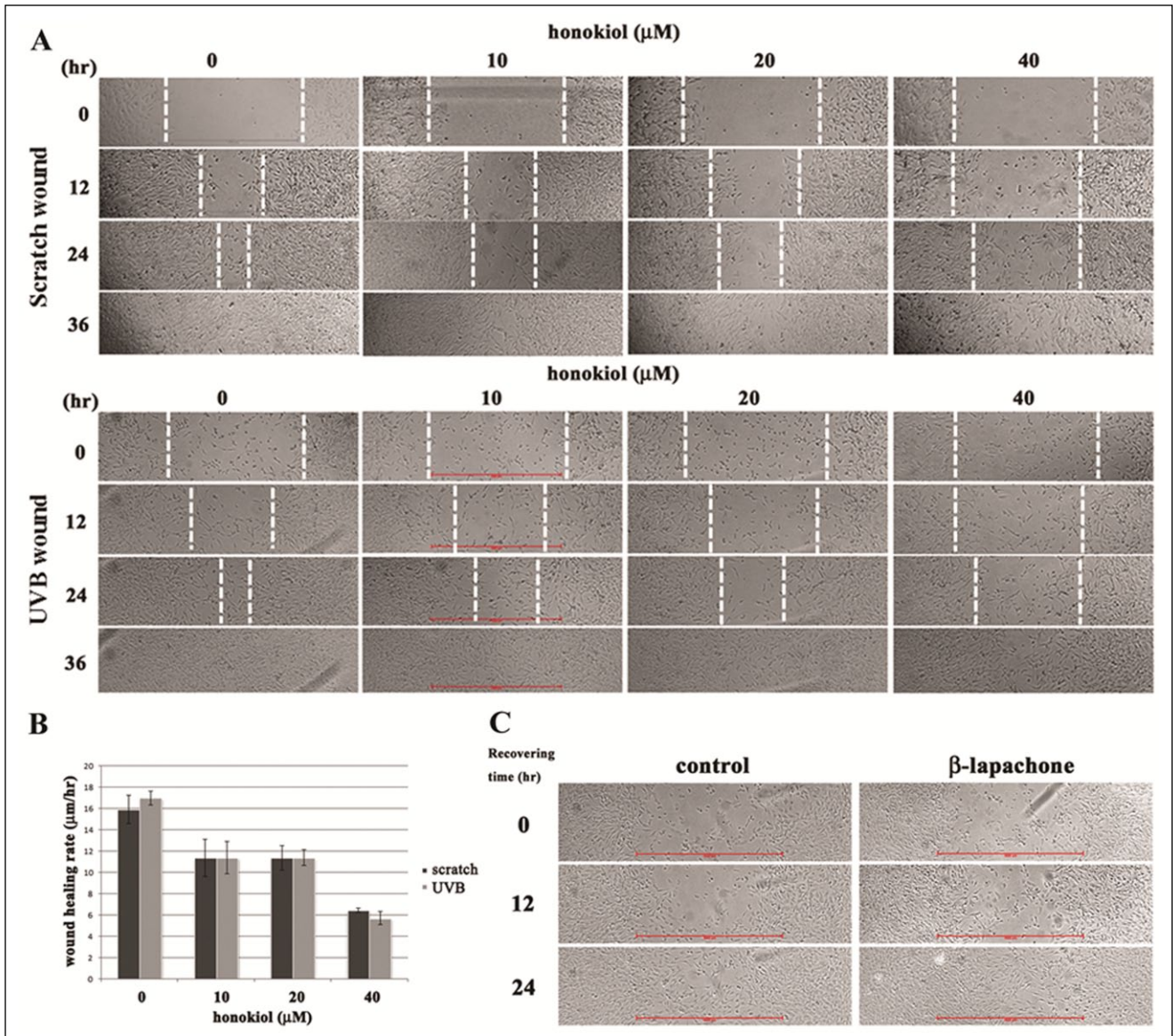


Figure 3. (A) Wound-healing processes in the scratch method (top) and the UVB method (bottom) before and after adding different concentrations of honokiol. Scale bar = 1 mm. (B) Wound-healing rates with standard error of the mean (SEM) plotted at different concentrations of honokiol. For each experimental condition three independent runs were performed to get the SEM. (C) Wound-healing processes in the UVB method without (left) and with (right) adding 2 μM β -lapachone. Scale bar = 1 mm.

increased as the result of adding β -lapachone, as clearly shown in **Figure 3C**.

In conclusion, in this article, we reported using UV lights to selectively kill cells and create a wound out of a cell monolayer. The potential limitations of this UV wound-healing assay are (1) one has to optimize the exposed UV dosage for every cell type to be studied, and (2) the boundary of the wound is not as sharp as those created using the scratch assay or the barrier assay. For all that, this method has advantages over traditional scratch and barrier wound-healing assays in its capability of creating wounds in various geometry shapes and being integrated with transparent

microfluidic chips. The latter makes the system suitable for long-term cellular studies under different environmental stimuli. Most important, combined with multiwell microplates and patterned masks, this method provides a high-throughput platform for simultaneously screening tens to hundreds of wound healing-related drugs.

Acknowledgments

We thank the Center for Emerging Material and Advanced Devices, National Taiwan University, for the cell culture room facility.

Declaration of Conflicting Interests

The authors declared no potential conflicts of interest with respect to the research, authorship, and/or publication of this article.

Funding

The authors disclosed receipt of the following financial support for the research, authorship, and/or publication of this article: This work is financially supported by the Ministry of Science and Technology of Taiwan under contract No. MOST 104-2311-B-002-026 (K. Y. Lo), No. MOST 104-2112-M-030-002 (Y. S. Sun), and National Taiwan University Career Development Project (NTU-CDP-103R7888) (K. Y. Lo).

References

- Friedl, P.; Gilmour, D. Collective Cell Migration in Morphogenesis, Regeneration and Cancer. *Nat. Rev. Mol. Cell Biol.* **2009**, *10*, 445–457.
- Rorth, P. Collective Cell Migration. *Annu. Rev. Cell Dev. Biol.* **2009**, *25*, 407–429.
- Weijer, C. J. Collective Cell Migration in Development. *J. Cell Sci.* **2009**, *122*, 3215–3223.
- Deisboeck, T. S.; Couzin, I. D. Collective Behavior in Cancer Cell Populations. *Bioessays* **2009**, *31*, 190–197.
- Friedl, P. Protease Requirements in Cancer Invasion In Vitro and In Vivo: From Individual to Collective Cell Migration. *Clin. Exp. Metastas.* **2007**, *24*, 227–227.
- Friedl, P.; Hegerfeldt, Y.; Tusch, M. Collective Cell Migration in Morphogenesis and Cancer. *Int. J. Dev. Biol.* **2004**, *48*, 441–449.
- Chen, H. C. Boyden Chamber Assay. *Methods Mol. Biol.* **2005**, *294*, 15–22.
- Li, Y. H.; Zhu, C. A Modified Boyden Chamber Assay for Tumor Cell Transendothelial Migration In Vitro. *Clin. Exp. Metastasis* **1999**, *17*, 423–429.
- Somersalo, K.; Salo, O. P.; Bjorksten, F.; et al. A Simplified Boyden Chamber Assay for Neutrophil Chemotaxis Based on Quantitation of Myeloperoxidase. *Anal. Biochem.* **1990**, *185*, 238–242.
- Jungi, T. W. Assay of Chemotaxis by a Reversible Boyden Chamber Eliminating Cell Detachment. *Int. Arch. Allergy Appl. Immunol.* **1975**, *48*, 341–352.
- Hasan, J.; Shnyder, S. D.; Bibby, M.; et al. Quantitative Angiogenesis Assays In Vivo—A Review. *Angiogenesis* **2004**, *7*, 1–16.
- Todaro, G. J.; Lazar, G. K.; Green, H. The Initiation of Cell Division in a Contact-Inhibited Mammalian Cell Line. *J. Cell Physiol.* **1965**, *66*, 325–333.
- Riahi, R.; Yang, Y.; Zhang, D. D.; et al. Advances in Wound-Healing Assays for Probing Collective Cell Migration. *J. Lab. Autom.* **2012**, *17*, 59–65.
- Yarrow, J. C.; Perlman, Z. E.; Westwood, N. J.; et al. A High-Throughput Cell Migration Assay Using Scratch Wound Healing, a Comparison of Image-Based Readout Methods. *BMC Biotechnol.* **2004**, *4*, 21.
- Goetsch, K. P.; Niesler, C. U. Optimization of the Scratch Assay for In Vitro Skeletal Muscle Wound Healing Analysis. *Anal. Biochem.* **2011**, *411*, 158–160.
- Fronza, M.; Geller, Z.; Bittencourt, C.; et al. The Scratch Assay: A Suitable In Vitro Tool for Studying Wound Healing Effects. *Planta Med.* **2008**, *74*, 1125–1126.
- Sun, Y. S.; Peng, S. W.; Cheng, J. Y. In Vitro Electrical-Stimulated Wound-Healing Chip for Studying Electric Field-Assisted Wound-Healing Process. *Biomicrofluidics* **2012**, *6*, 34117.
- Simpson, M. J.; Treloar, K. K.; Binder, B. J.; et al. Quantifying the Roles of Cell Motility and Cell Proliferation in a Circular Barrier Assay. *J. R. Soc. Interface* **2013**, *10*, 20130007.
- Kroening, S.; Goppelt-Struebe, M. Analysis of Matrix-Dependent Cell Migration with a Barrier Migration Assay. *Sci. Signal.* **2010**, *3*, p11.
- Block, E. R.; Matela, A. R.; SundarRaj, N.; et al. Wounding Induces Motility in Sheets of Corneal Epithelial Cells through Loss of Spatial Constraints. *J. Biol. Chem.* **2004**, *279*, 24307–24312.
- Nikolić, D. L.; Boettiger, A. N.; Bar-Sagi, D.; et al. Role of Boundary Conditions in an Experimental Model of Epithelial Wound Healing. *Am. J. Physiol. Cell Physiol.* **2006**, *291*, C68–C75.
- van Horsen, R.; Galjart, N.; Rens, J. A. P.; et al. Differential Effects of Matrix and Growth Factors on Endothelial and Fibroblast Motility: Application of a Modified Cell Migration Assay. *J. Cell. Biochem.* **2006**, *99*, 1536–1552.
- Zordan, M. D.; Mill, C. P.; Riese, D. J.; et al. A High Throughput, Interactive Imaging, Bright-Field Wound Healing Assay. *Cytom. Part A* **2011**, *79*, 227–232.
- Keese, C. R.; Wegener, J.; Walker, S. R.; et al. Electrical Wound-Healing Assay for Cells In Vitro. *Proc. Natl. Acad. Sci. U. S. A.* **2004**, *101*, 1554–1559.
- Murrell, M.; Kamm, R.; Matsudaira, P. Tension, Free Space, and Cell Damage in a Microfluidic Wound Healing Assay. *PLoS One* **2011**, *6*, e24283.
- Naik, E.; Michalak, E. M.; Villunger, A.; et al. Ultraviolet Radiation Triggers Apoptosis of Fibroblasts and Skin Keratinocytes Mainly via the BH3-Only Protein Noxa. *J. Cell. Biol.* **2007**, *176*, 415–424.
- Xu, H. X.; Yan, Y.; Li, L.; et al. Ultraviolet B-Induced Apoptosis of Human Skin Fibroblasts Involves Activation of Caspase-8 and -3 with Increased Expression of Vimentin. *J. Dermatol.* **2010**, *37*, 109–109.
- Gentile, M.; Latonen, L.; Laiho, M. Cell Cycle Arrest and Apoptosis Provoked by UV Radiation-Induced DNA Damage Are Transcriptionally Highly Divergent Responses. *Nucleic Acids Res.* **2003**, *31*, 4779–4790.
- Shen, Y. H.; Devgan, G.; Darnell, J. E.; et al. Constitutively Activated Stat3 Protects Fibroblasts from Serum Withdrawal and UV-Induced Apoptosis and Antagonizes the Proapoptotic Effects of Activated Stat1. *Proc. Natl. Acad. Sci. U. S. A.* **2001**, *98*, 1543–1548.
- Matta, J. L.; Ramos, J. M.; Armstrong, R. A.; et al. Environmental UV-A and UV-B Threshold Doses for Apoptosis and Necrosis in Human Fibroblasts. *Photochem. Photobiol.* **2005**, *81*, 563–568.
- Hulkower, K.; Herber, R. Cell Migration and Invasion Assays as Tools for Drug Discovery. *Pharmaceutics* **2011**, *3*, 107–142.

32. Lo, K. Y.; Zhu, Y.; Tsai, H. F.; et al. Effects of Shear Stresses and Antioxidant Concentrations on the Production of Reactive Oxygen Species in Lung Cancer Cells. *Biomicrofluidics* **2013**, *7*, 64108.
33. Wu, S. Y.; Hou, H. S.; Sun, Y. S.; et al. Correlation between Cell Migration and Reactive Oxygen Species under Electric Field Stimulation. *Biomicrofluidics* **2015**, *9*, 054120.
34. Lo, K. Y.; Wu, S. Y.; Sun, Y. S. A Microfluidic Device for Studying the Production of Reactive Oxygen Species and the Migration in Lung Cancer Cells under Single or Coexisting Chemical/Electrical Stimulation. *Microfluid. Nanofluid.* **2016**, *20*, 15.
35. Treloar, K. K.; Simpson, M. J.; McElwain, D. L.; et al. Are In Vitro Estimates of Cell Diffusivity and Cell Proliferation Rate Sensitive to Assay Geometry? *J. Theor. Biol.* **2014**, *356*, 71–84.
36. Singh, T.; Katiyar, S. K. Honokiol Inhibits Non–Small Cell Lung Cancer Cell Migration by Targeting PGE(2)-Mediated Activation of Beta-Catenin Signaling. *PLoS One* **2013**, *8*, e60749.
37. Singh, T.; Prasad, R.; Katiyar, S. K. Inhibition of Class I Histone Deacetylases in Non–Small Cell Lung Cancer by Honokiol Leads to Suppression of Cancer Cell Growth and Induction of Cell Death In Vitro and In Vivo. *Epigenetics* **2013**, *8*, 54–65.
38. Kung, H. N.; Yang, M. J.; Chang, C. F.; et al. In Vitro and In Vivo Wound Healing-Promoting Activities of Beta-Lapachone. *Am. J. Physiol. Cell Physiol.* **2008**, *295*, C931–C943.